GEOPHYSICAL RESEARCH LETTERS, VOL. 36, L14106, doi:10.1029/2009GL038980, 2009

Click Here for Full Article

THEMIS observations of an earthward-propagating dipolarization front

A. Runov,[1] V. Angelopoulos,[1] M. I. Sitnov,[2] V. A. Sergeev,[3] J. Bonnell,[4] J. P. McFadden,[4] D. Larson,[4] K.-H. Glassmeier,[5,6] and U. Auster[5]

Received 30 April 2009; revised 22 June 2009; accepted 26 June 2009; published 29 July 2009.

[1] We report THEMIS observations of a dipolarization front, a sharp, large-amplitude increase in the *Z*-component of the magnetic field. The front was detected in the central plasma sheet sequentially at X = −20.1 R_E (THEMIS P1 probe), at X = −16.7 R_E (P2), and at X = −11.0 R_E (P3/P4 pair), suggesting its earthward propagation as a coherent structure over a distance more than 10 R_E at a velocity of 300 km/s. The front thickness was found to be as small as the ion inertial length. Comparison with simulations allows us to interpret the front as the leading edge of a plasma fast flow formed by a burst of magnetic reconnection in the midtail.
Citation: Runov, A., V. Angelopoulos, M. I. Sitnov, V. A. Sergeev, J. Bonnell, J. P. McFadden, D. Larson, K.-H. Glassmeier, and U. Auster (2009), THEMIS observations of an earthward-propagating dipolarization front, *Geophys. Res. Lett.*, *36*, L14106, doi:10.1029/2009GL038980.

1. Introduction

[2] Spatially and temporally localized dipolarizations (increases in magnetic field elevation angle) are often observed in the near-Earth and in the mid-tail plasma sheet during bursty bulk flow (BBF) events. Recent superposed epoch analyses based on Geotail data reveal similarity in BBF-related variations of the north−south magnetic field component (B_z), ion density and temperature observed at $-31 < X < -5$ R_E [*Ohtani et al.*, 2004]. Transient dipolarizations, observed near the leading edge of fast flows, include a sharp increase of B_z (a dipolarization front, DF), preceded by a smaller amplitude negative B_z variation.

[3] Dipolarizations, observed in the near-Earth plasma sheet at $X \sim -10$ R_E, are often interpreted as signatures of magnetic flux pileup [*Hesse and Birn*, 1991; *Baumjohann et al.*, 1999; *Shiokawa et al.*, 1997]. They may also result from a current-driven instability (current disruption) [*Lui et al.*, 1988]. The latter concept explains the negative B_z variation prior to DF as temporal thinning of the cross-tail current sheet (explosive growth phase) [*Ohtani et al.*, 1992]. Transient dipolarizations observed in the mid-tail plasma sheet are interpreted either as BBF-type flux ropes [*Slavin et al.*, 2003] or as Nightside Flux Transfer Events [*Sergeev et al.*, 1992]. The former interpretation is based on the multiple X-line concept; the latter is supported by an MHD model of transient fast reconnection [e.g., *Semenov et al.*, 2005]. Both models interpret the negative B_z variation as a spatial structure. Recent PIC simulations with open boundary conditions [*Sitnov et al.*, 2009] have confirmed that distinctive DF features, including a small B_z dip, steep front-like buildup of the northward magnetic field, and fast propagation of that front structure over a long distance (several R_E), may all be explained by transient reconnection in the magnetotail. To understand the physics of the DF formation, it is important to follow DF structure over a long distance and distinguish between spatial and temporal variations.

[4] In this paper we report on DF observations by five THEMIS spacecraft (probes) situated in the near-equatorial plasma sheet at distances of $-20 < X < -10$ R_E. Data from the Flux-gate Magnetometer (FGM) [*Auster et al.*, 2008], Electric Field Instrument (EFI) [*Bonnell et al.*, 2008], Electrostatic Analyzer (ESA) [*McFadden et al.*, 2008], and Solid State Telescope (SST) [*Angelopoulos*, 2008] are used in this study.

2. Observations

[5] We discuss THEMIS observations between 0745 and 0805 UT on Feb. 27, 2009. According to OMNI data (not shown), IMF B_z at 1 AU was mainly northward between 0130 and 0710 UT, southward between 0710 and 0725 UT, northward between 0725 and 0748 UT, and turned southward at 0749 UT. THEMIS pseudo-AE (calculated using the THEMIS ground-based magnetometer array [*Russell et al.*, 2008; *Mann et al.*, 2008]) began to gradually increase at ∼0720 UT and experienced a rapid increase from ∼60 nT to ∼200 nT between 0750 and 0800 UT (THEMIS-AE data are available at http://themis.ssl.berkeley.edu/summary.shtml).

[6] Figure 1 shows the locations of the THEMIS probes in *XY* and *XZ* GSM planes at 0752 UT and the time series of the Z_{GSM} component of the magnetic field (4 vectors/s resolution) at all five probes. Coordinates of the two distant probes, P1 (THB) and P2 (THC), were [20.1, −0.6, −1.5] R_E and [−16.7, −1.6, −2.2] R_E, respectively. The innermost probes were at P4(THE): [−11.1, −1.8, −2.4], P3(THD): [−11.1, −2.8, −2.1], and P5(THA): [−11.0, −1.9, −3.3] R_E.

[7] Between 0751 and 0754 UT, similar, front-like variations in B_z were detected consecutively by the P1, P2, and

[1]Institute of Geophysics and Planetary Physics, University of California, Los Angeles, California, USA.
[2]Johns Hopkins University Applied Physics Laboratory, Laurel, Maryland, USA.
[3]St. Petersburg State University, St. Petersburg, 198504, Russia.
[4]Space Science Laboratory, University of California, Berkeley, California, USA.
[5]Institute of Geophysics and Extraterrestrial Physics, Technical University Braunschweig, Braunschweig, Germany.
[6]Max Planck Institute for Solar System Research, Katlenburg-Lindau, Germany.

Copyright 2009 by the American Geophysical Union.
0094-8276/09/2009GL038980$05.00

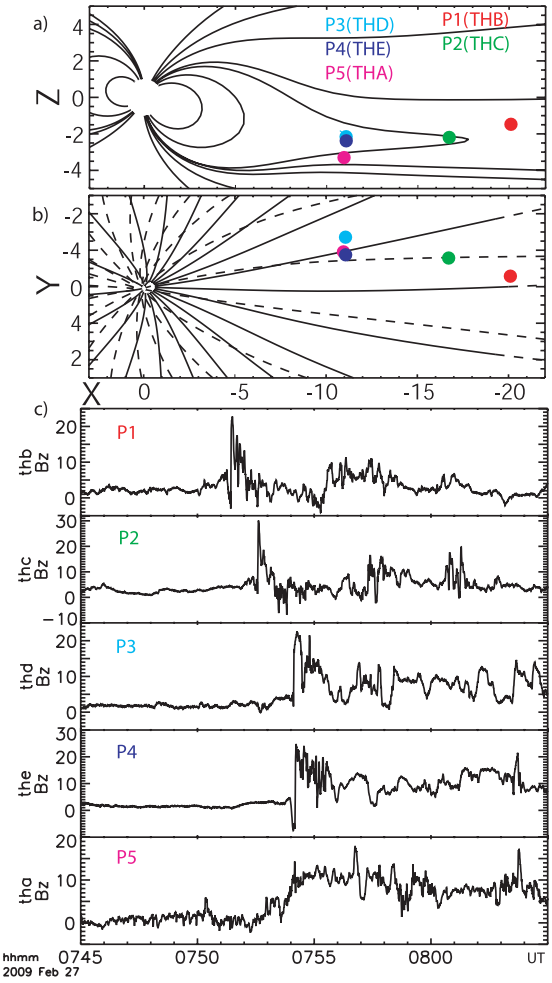

Figure 1. THEMIS SC positions in (a) *XZ* and (b) *XZ* GSM planes. T96-model magnetic field [*Tsyganenko*, 1995] is shown. (c) Time series of B_z (GSM) at all five probes (P1–P5).

P3/P4 probes (Figure 1c), with a more gradual buildup of B_z at P5, which was located 1 R_E southward of P3/P4. Assuming a planar front, the timing of the DF at P1 (0751:26 UT) and P2 (0752:35 UT) suggests earthward propagation at a velocity of 330 km/s. Timing at P2 and P4 (0754:10 UT) results in 360 km/s. Thus, the DF propagates from −20 to −11 R_E without deceleration.

[8] Figure 2 summarizes observations at P1 and P2 for 2.5 min around the DF (0751:00–0752:30 UT and 0752:00–0753:30 UT, respectively). P1 and P2 were in northern and southern halves of the plasma sheet, respectively, close to the neutral sheet. Between 0751:15 and 0751:30 UT, P1/FGM detected a bipolar (negative then positive) variation in the B_x (blue trace) and B_z components (red trace), accompanied by a positive variation in B_y. Since the burst-mode survey was triggered by the variation of B_z, FGM data with the highest time resolution (FGH, 128 vectors/s) are available. Using FGH data, the precise duration of the front passage from negative B_z peak (−5 nT) to the first local positive peak (20 nT) was shown to be 1.35 s, (Figure 2c), i.e., the DF thickness was ≃400 km. The electric field components E_y and E_x, shown in the GSE coordinates, registered by P1/EFI, increased on the DF. The time-energy spectrograms show rapid changes indicating ion and electron energization. Plasma moments reveal a drop in plasma density and pressure (P_p) accompanied by a gradual increase in earthward bulk flow speed up to 1000 km/s and an increase in magnetic pressure (P_m).

[9] P2, located 3.4 R_E earthward of P1, detected bipolar (small-amplitude negative then sharp, high-amplitude positive) variations in $|B_x|$ and B_z between 0751:25 and 0752:35 UT. They were associated with a positive B_y variation, an increase in E_x and E_y, rapid changes in particle ET spectra, a drop in ion density, and an increase in earthward plasma flow. During the negative B_z variation, P_p increased while P_m decreased (this effect is more pronounced at P2 than at P1). At the DF, P_p rapidly decreased while P_m quickly rose. Peak-to-peak (1.5 and 31 nT) front propagation time was estimated using FGH data (Figure 2d) to be 1.70 s, i.e., the DF was 500 km thick.

[10] Figure 3 shows DF observations at P3 and P4 situated at the same X and Z and separated by 1 R_E in Y_{GSM}. At 0753:30 UT, both P3 and P4 were in the southern half of the plasma sheet at B_x = −25 and −22 nT, respectively, detecting B_z = 3 nT. At 0753:50 UT, P3 started to detect a decrease in $|B_x|$ and $|B_y|$ without significant variations in B_z. A sharp decrease in B_z down to zero was observed between 0754:06.0 and 0754:06.5 UT. Both $|B_x|$ and $|B_y|$ reached local minima in that interval, resulting in $|B|$ = 2.3 nT. At 0754:08.1 UT, B_z reached a local maximum (19 nT). The DF passing time (1.6 s, Figure 3c) corresponds to a thickness of 500 km. P4 started to detect a decrease in B_z and an increase in B_y at 0753:57 UT. A local minimum in B_z (−8 nT) was detected at 0754:10.3 UT, and a local B_z maximum (26 nT) at 0754:12.0 UT (1.7 s front passage duration, 500 km thickness). Variations in magnetic field, particle spectra and moments detected by P3 and P4 are similar to those detected earlier by P1 and P2, which suggests that the probes encountered the same spatial structure.

[11] Observations made by P5, located at the same X and Y as P4 but 1 R_E southward, between 0752:30 and 0755:00 UT are summarized in Figure 4. Although P5 observed more gradual dipolarization (see also Figure 1), the signatures in spectra, moments and magnetic pressure at P5 were similar to those at the other probes. They started earlier compared to P3/P4, presumably because P5 was farther from the neutral plane (B_x = −36 nT at 0752:30 UT). The time-delay between increases in P_m at P1 and P5 (92 s) gives a propagation velocity of 400 km/s.

Figure 2. Summary of THEMIS (a) P1 and (b) P2 observations between 0750:30 and 0755:00 UT. For each probe, *X*, *Y*, and *Z* GSM components of the magnetic field, *X* and *Y* GSE components of the electric field (spin resolution), ion energy-time spectrogram (eV/s/cm^2/eV) combining SST and ESA ions (a blank stripe indicates the energy gap between the two instrument ranges), electron (SST and ESA) time-energy spectrogram, ion number density *X*, *Y*, and *Z* GSM components of the ion bulk velocity calculated with ESA and SST inputs, magnetic (P_m) and plasma (P_p) pressures are shown. (c) and (d) GSM **B** (128 vectors/s) during 15 s around the dipolarization front at P1 and P2, respectively.

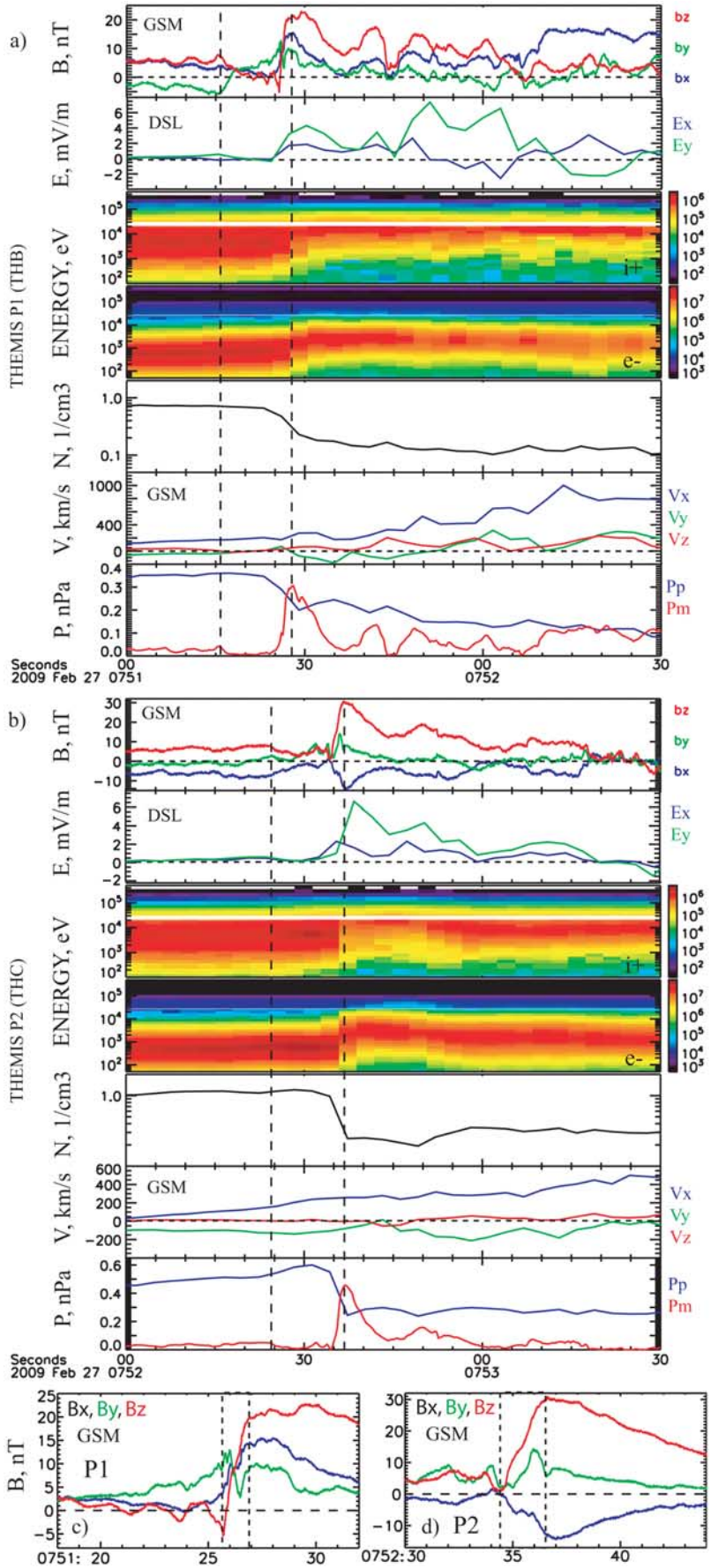
a)
B, nT
GSM
bz
by
bx
E, mV/m
DSL
Ex
Ey
THEMIS P1 (THB)
ENERGY, eV
i+
e-
N, 1/cm3
V, km/s
GSM
Vx
Vy
Vz
P, nPa
Pp
Pm
Seconds
2009 Feb 27 0751
00
30
0752
b)
THEMIS P2 (THC)
2009 Feb 27 0752
0753
c)
P1
0751: 20
25
30
Bx, By, Bz
GSM
d) P2
0752:30
35
40

Figure 2

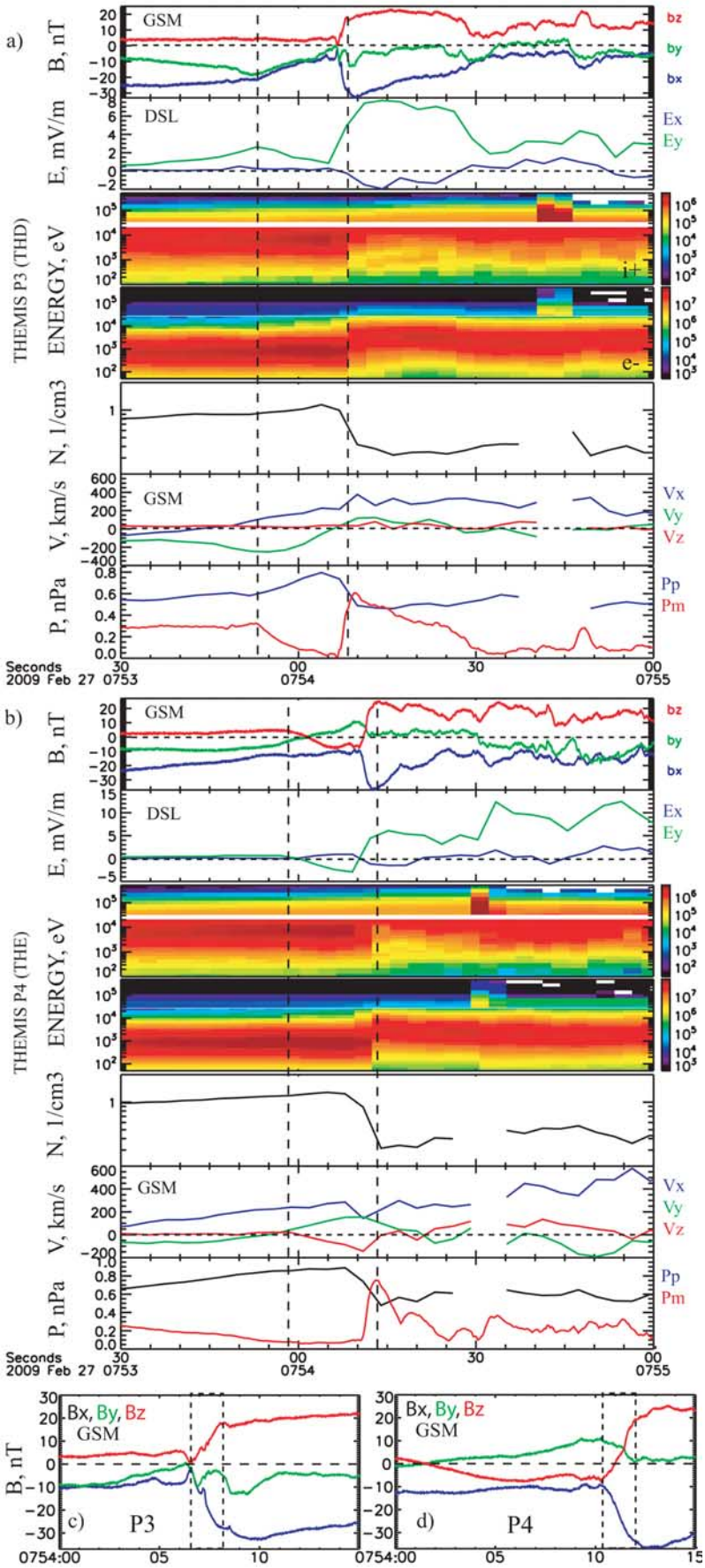

Figure 3. Summary of THEMIS P3 and P4 observations during 0750:30–0755:00 UT. The same format as in Figure 2.

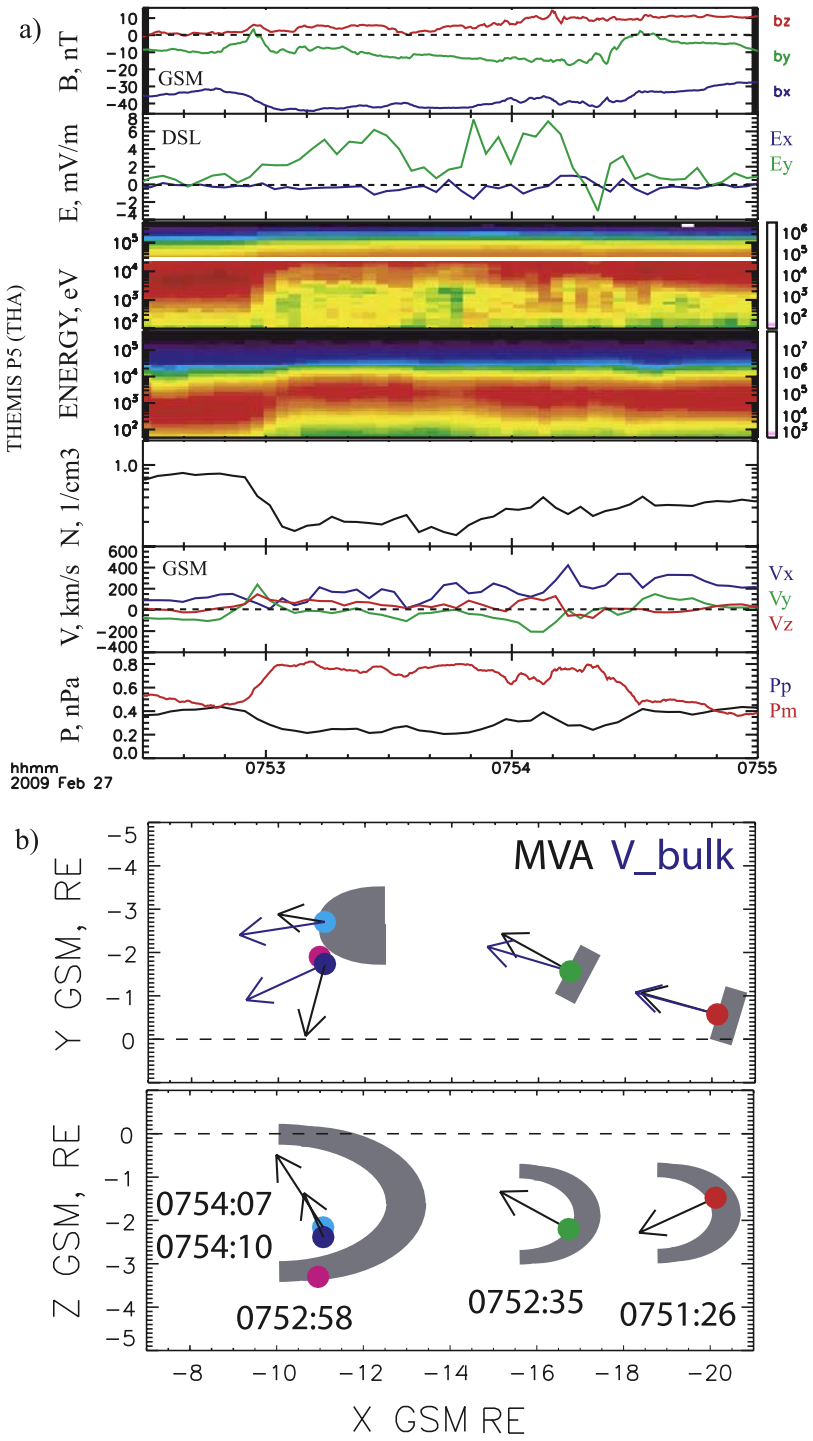

Figure 4. (a) Summary of THEMIS P5 observations between 0752:30 and 0755:00 UT. The same format as in Figure 2. (b) An interpretation scheme. Black arrows are projections of MVA normals (R_1) onto (top) *XY* and (bottom) *XZ* GSM planes; blue arrows are projections of bulk velocity directions to the *XY* GSM plane. Gray segments represent a flux tube with the enhanced magnetic flux populated by hot, tenuous plasma. Times of DF crossing by each probe are shown.

[12] To determine the front orientation the Minimum Variance Analysis (MVA) [*Sonnerup and Scheible*, 1998] was applied to the magnetic field time series at four probes (P1–P4) detecting the DF. The MVA results are summarized in Table 1. The three MVA eigenvectors, $\mathbf{R}_1$, $\mathbf{R}_2$, and $\mathbf{R}_3$, corresponding to the three eigenvalues, λ_1, λ_2, and λ_3 define maximum, intermediate, and minimum variance directions in the GSM coordinates, respectively. To define the direction unambiguously, the *X*-component of the minimum variance direction was set to be positive (earthward) in accord with the propagation direction defined from timing. $\mathbf{R}_3$ may be interpreted as the front-normal vector.

Table 1. Minimum Variance Analysis Results[a]

sc	UT	λ_1, λ_2, λ_3,	R_1	R_2	R_3
P1	0751:26	76.5, 6.02, 0.13	0.37,−0.16, 0.91	−0.29,−0.95,−0.05	0.88,−0.25,−0.40
P2	0752:35	107.0, 8.93, 0.17	0.35,−0.26, 0.90	−0.50,−0.86,−0.05	0.79,−0.43,−0.43
P3	0754:07	102.3, 4.64, 0.72	0.83,0,−0.08,−0.55	0.12, 0.99, 0.03	0.54,−0.09, 0.84
P4	0754:11	153.2, 1.90,0.04	0.69, 0.24,−0.69	0.69,−0.50, 0.52	0.22, 0.83, 0.51

[a]UT indicates instances of the center of the positive B_z variations. MVA was performed over a variable window around the specified UT. Results with the best ratio of λ_2 and λ_3 are shown.

At P1 and P2, the normals were close to the *X* direction, indicating a boundary in the *YZ* plane. The bulk velocity directions were close to the normals (Figure 4b). At P3 and P4, the *XZ* projections of normals were consistent, while *XY* projections were almost orthogonal. The normal at P3 indicates a tilt of the front in the *XZ* plane. Projections of bulk velocity directions at P3 and P4 were similar. We did not apply MVA to P5 data in view of rather gradual magnetic field variations there.

3. Discussion and Summary

[13] Multi-point observations by the five THEMIS probes between 0751 and 0755 UT on Feb. 27, 2009 provide the first unambiguous evidence of the earthward propagation of a dipolarization front (DF) from tailward of 20 R_E to 11 R_E at a speed of 300 km/s. The DF separated different plasma populations. The front thickness was 400–500 km, comparable to the ion inertial length ($d_i \sim 300$ km for 0.5 cm^{-3}) and the 3.5 keV (the ion temperature ahead of the front) ion gyroradius in $B_z = 20$ nT (400 km).

[14] Variations in magnetic field and plasma moments at the DF reveal characteristic signatures of BBFs [*Angelopoulos et al.*, 1992]: increase in bulk velocity and magnetic pressure, and decrease in plasma density and pressure. These are also predicted by the plasma bubble model [e.g., *Birn et al.*, 2004, and references therein]. The bubble concept helps explain the delay in disturbance detection at P4, compared to P5 located 1 R_E southward, by the sharply curved shape of the corresponding depleted flux tube, consistent both with the MHD simulations [*Birn et al.*, 2004] and with observations [*Nakamura et al.*, 2005]. The effect may be enhanced by faster propagation of disturbances at the plasma sheet periphery, where the Alfvén speed is larger than at the neutral plane [e.g., *Krauss-Varban and Karimabadi*, 2003]. Figure 4b summarizes the observation and interpretation scheme. The MVA normal directions suggest that the dipolarization region was deflected dawnward, consistent with earlier observations [*Nakamura et al.*, 2002], so that P4 was eventually found on its dusk-side edge.

[15] Our observations show that the quick southward variation observed ahead of the DF is a spatial structure associated with the propagating dipolarization front. The observed spatial scales of the DF and the B_z-dip ($\sim d_i$) are similar to those resulting from PIC simulations [*Sitnov et al.*, 2009]. This scale suggests a relation to the Hall-type currents due to ion-electron decoupling on the front. The corresponding E_x was found in the simulations and in the data. The short ($\sim$1 s) B_z dips were preceded by a longer decrease in magnetic pressure and simultaneous increase in plasma pressure, indicating a diamagnetic effect due to plasma compression ahead of the DF.

[16] To conclude, observations with the conjunction of the THEMIS probes stretched along the magnetotail reveal an example of space plasma self-organization, when a micro-scale structure, with thickness of the ion inertial scale implying different motions of ions and electrons, remains structurally stable during its propagation over a macroscopic distance of about 10 R_E. The analysis of such thin boundaries requires a kinetic approach. The agreement with PIC simulations [*Sitnov et al.*, 2009] suggests transient magnetic reconnection as the most plausible source of DFs in the magnetotail.

[17] **Acknowledgments.** We acknowledge NASA contracts NAS5-02099 and NNX08AD85G, the German Ministry for Economy and Technology and the German Center for Aviation and Space (DLR), contract 50 OC 0302. The OMNI data are available on CDAWeb. We thank P. L. Pritchett and L. Lyons for discussions, and B. Kerr, P. Cruce, A. Prentice, and J. Hohl for help with software and editing.

References

Angelopoulos, V. (2008), The THEMIS mission, *Space Sci. Rev.*, *141*, 5–34.

Angelopoulos, V., W. Baumjohann, C. F. Kennel, F. V. Coroniti, M. G. Kivelson, R. Pellat, R. J. Walker, H. Lhr, and G. Paschmann (1992), Bursty bulk flows in the inner central plasma sheet, *J. Geophys. Res.*, *97*, 4027–4039.

Auster, H. U., et al. (2008), The THEMIS fluxgate magnetometer, *Space Sci. Rev.*, *141*, 235–264.

Baumjohann, W., M. Hesse, S. Kokubun, T. Mukai, T. Nagai, and A. A. Petrukovich (1999), Substorm dipolarization and recovery, *J. Geophys. Res.*, *104*, 24,995–25,000.

Birn, J., J. Raeder, Y. L. Wang, R. A. Wolf, and M. Hesse (2004), On the propagation of bubbles in the geomagnetic tail, *Ann. Geophys.*, *22*, 1773–1786.

Bonnell, J. W., et al. (2008), The electric field instrument (EFI) for THEMIS, *Space Sci. Rev.*, *141*, 303–341.

Hesse, M., and J. Birn (1991), On reconnection and its relation to the substorm current wedge, *J. Geophys. Res.*, *96*, 19,417–19,426.

Krauss-Varban, D., and H. Karimabadi (2003), Timing and localization of reconnection signatures: Is there a substorm model problem?, *Geophys. Res. Lett.*, *30*(6), 1308, doi:10.1029/2002GL016369.

Lui, A. T. Y., R. E. Lopez, S. M. Krimigis, R. W. McEntire, and L. J. Zanetti (1988), A case study of magnetotail current sheet disruption and diversion, *Geophys. Res. Lett.*, *15*, 721–724.

Mann, I. R., et al. (2008), The upgraded CARISMA magnetometer array in the THEMIS era, *Space Sci. Rev.*, *141*, 413–451.

McFadden, J. P., et al. (2008), The THEMIS ESA plasma instrument and in-flight calibration, *Space Sci. Rev.*, *141*, 277–302.

Nakamura, R., et al. (2002), Motion of the dipolarization front during a flow burst event observed by Cluster, *Geophys. Res. Lett.*, *29*(20), 1942, doi:10.1029/2002GL015763.

Nakamura, R., et al. (2005), Multi-point observation of the high-speed flows in the plasma sheet, *Adv. Space. Res.*, *36*, 1444–1447.

Ohtani, S., S. Kokubun, and C. T. Russell (1992), Radial expansion of the tail current disruption during substorms: A new approach to the substorm onset region, *J. Geophys. Res.*, *97*, 3129–3136.

Ohtani, S. I., M. A. Shay, and T. Mukai (2004), Temporal structure of the fast convective flow in the plasma sheet: Comparison between observations and two-fluid simulations, *J. Geophys. Res.*, *109*, A03210, doi:10.1029/2003JA010002.

Russell, C. T., et al. (2008), THEMIS ground-based magnetometers, *Space Sci. Rev.*, *141*, 389–412.

Semenov, V. S., et al. (2005), Reconstruction of the reconnection rate from Cluster measurements: First results, *J. Geophys. Res.*, *110*, A11217, doi:10.1029/2005JA011181.

Sergeev, V., R. C. Elphic, F. S. Mozer, A. Saint-Marc, and J.-A. Sauvaud (1992), A two-satellite study of nightside flux transfer events in the plasma sheet, *Planet. Space Sci.*, *40*, 1551–1572.

Shiokawa, K., W. Baumjohann, and G. Haerendel (1997), Braking of high-speed flows in the near-Earth tail, *Geophys. Res. Lett.*, *24*, 1179–1182.

Sitnov, M. I., M. Swisdak, and A. V. Divin (2009), Dipolarization fronts as a signature of transient reconnection in the magnetotail, *J. Geophys. Res.*, *114*, A04202, doi:10.1029/2008JA013980.

Slavin, J. A., R. P. Lepping, J. Gjerloev, D. H. Fairfield, M. Hesse, C. J. Owen, M. B. Moldwin, T. Nagai, A. Ieda, and T. Mukai (2003), Geotail observations of magnetic flux ropes in the plasma sheet, *J. Geophys. Res.*, *108*(A1), 1015, doi:10.1029/2002JA009557.

Sonnerup, B. U. Ö., and M. Scheible (1998), Minimum and maximum variance analysis, in *Analysis Methods for Multi-Spacecraft Data*, edited by G. Paschmann and P. Daly, pp. 185–220, Eur. Space Agency, Noordwijk, Netherlands.

Tsyganenko, N. A. (1995), Modeling the Earth's magnetospheric magnetic field confined within a realistic magnetopause, *J. Geophys. Res.*, *100*, 5599–5612.

V. Angelopoulos and A. Runov, Institute of Geophysics and Planetary Physics, University of California, Los Angeles, CA 90095, USA. (arunov@igpp.ucla.edu)

U. Auster and K.-H. Glassmeier, Institute of Geophysics and Extraterrestrial Physics, Technical University Braunschweig, D-38106 Braunschweig, Germany.

J. Bonnell, D. Larson, and J. P. McFadden, Space Science Laboratory, University of California, Berkeley, CA 94720, USA.

V. A. Sergeev, St. Petersburg State University, St. Petersburg 198504, Russia.

M. I. Sitnov, Johns Hopkins University Applied Physics Laboratory, Laurel, MD 20723–6099, USA.